Fast ionic diffusion in Li_2S investigated by quasielastic neutron scattering

1994 J. Phys.: Condens. Matter 6 9937

(http://iopscience.iop.org/0953-8984/6/46/012)

J. Phys.: Condens. Matter 6 (1994) 9937–9947. Printed in the UK

Fast ionic diffusion in Li_2S investigated by quasielastic neutron scattering

F Altorfer†‖, W Bührer†, I Anderson‡, O Schärpf‡, H Bill§ and P L Carron§

† Laboratory for Neutron Scattering ETHZ&PSI, CH-5232 Villigen PSI, Switzerland

‡ Institute Laue Langevin, F-38042 Grenoble Cédex 9, France

§ Département de Chimie Physique, Quai E Ansermet 30, CH-1211 Geneva, Switzerland

Received 21 April 1994, in final form 2 September 1994

Abstract. The Li diffusion in Li_2S at high temperatures was investigated by quasielastic neutron scattering techniques on a single crystal of $^7Li_2S$. It is shown by using polarized neutrons that the scattering is almost purely incoherent. The data were analysed in terms of an extended Chudley–Elliott jump diffusion model. The Li diffusion process takes place by hopping between regular tetrahedral and interstitial octahedral sites. The mean residence times on the regular Li sites were estimated to be 17.3 ps at $T = 1173$ K, 6.7 ps at 1273 K and 4.3 ps at 1363 K.

1. Introduction

Lithium sulphide (Li_2S) crystallizes in the antifluorite structure (space group $Fm3m$), which provides one of the simplest systems in which fast ionic conduction can be observed. The crystal structure can be considered as a simple cubic array of Li^+ ions (with half of the FCC lattice constant) where every second cube is centred by an S^{2-} ion (figure 1). Fluorites and antifluorites have attracted much attention due to their high-temperature properties. They undergo a diffuse phase transition to a fast ionic conductive state in the temperature range of $T_F = (0.6\text{–}0.8)T_{melt}$. The melting point of Li_2S is 1645 K and electrical conductivity experiments [1], neutron diffraction experiments [2] and Brillouin scattering [3] show that the diffuse phase transition sets in at $T_F \sim 800$ K. The low ratio of T_F/T_{melt} allows the disordered state in Li_2S to be observed over a wide temperature range. The analysis of the neutron diffraction patterns showed that approximately 15% of the Li^+ ions are on octahedral interstitial sites at $T = 1300$ K. It is expected that the diffusion process would give rise to quasielastic scattering [4] providing information about jump rates and jump vectors of the mobile ion.

2. Experimental details

Since Li in its natural composition has a rather high absorption cross-section for thermal neutrons, an isotopically pure ^7Li single crystal was grown. The single crystal had a mosaic of 0.4° and was of cylindrical form (1.2 cm in diameter, 3 cm in length). Details of the sample preparation have been described by Carron [1]. Since Li_2S is very hygroscopic the single crystal was sealed in a Pt container.

‖ Present address: Reactor Radiation Division, National Institute of Standards and Technology, Gaithersburg, MD-20899, USA.

0953-8984/94/469937+11$19.50

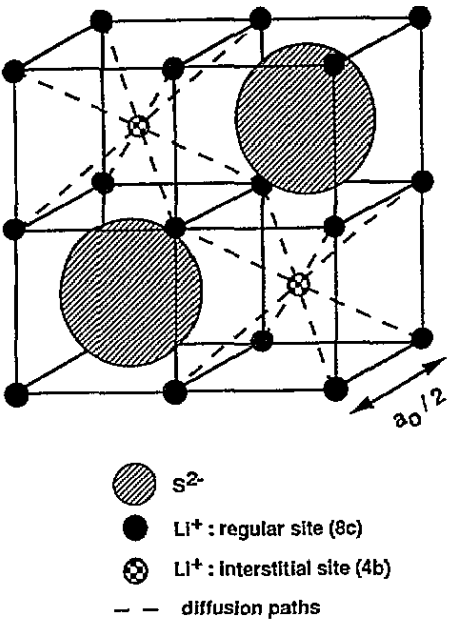

Figure 1. The crystal structure of Li_2S (space group $Fm3m$); for clarity only half of the unit cell is shown. Possible Li^+ diffusion paths between tetrahedral (8c) and octahedral (4b) sites are indicated by dashed lines.

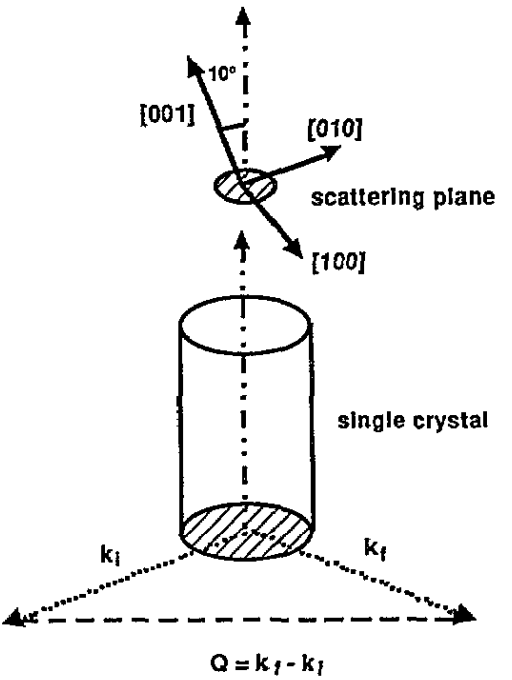

Figure 2. The single-crystal orientation of scattering experiments on instrument D7.

2.1. Measurements with polarization analysis

In principle, since the incoherent and the coherent cross-sections of ^7Li are of similar magnitude ($\sigma_{coh}(^7Li) = 0.619$ barns, $\sigma_{incoh}(^7Li) = 0.68$ barns [5]), the quasielastic scattering from the Li ion may consist of incoherent and coherent components, which determine single-particle and correlated motions, respectively. For an isotopically pure sample these two components can be separated by analysing the spin state of the neutron before and after the scattering process. Whereas coherent scattering occurs with no change of the neutron spin (non-spin flip), incoherent scattering occurs with a probability of $\frac{1}{3}$ without and $\frac{2}{3}$ with change of the spin state (spin flip) [6]. This enables us to distinguish between incoherent and coherent scattering by subtracting half of the spin flip intensity from the non-spin flip intensity in order to obtain the true coherent contribution in the non-spin flip signal.

In order to check whether the quasielastic scattering at high temperatures stems from a coherent or an incoherent scattering process, experiments were performed on the time of flight (TOF) spectrometer D7 [7] at the ILL using polarization analysis. The spectra were measured with an incoming wavelength of 4.8 Å (200 μeV energy resolution) at temperatures of 300 K and 1173 K. The orientation of the single crystal during the experiment is displayed in figure 2. The [001] axis had an orientation of approximately 10° relative to the normal of the scattering plane. The orientation of the [010] axis relative to the wavevector k_i of the incoming neutrons is sketched. The polarization analysis data taken on D7 (shown at a particular Q in figure 3) indicate that the measured intensity is mainly incoherent. Furthermore elastic scans over a representative zone in reciprocal space (obtained by rotating the single crystal) showed that the diffuse intensity was approximately

constant as would be expected in the case of no correlation between interstitials. In this case the coherent diffuse scattering is given by the Laue term; at 1173 K (with $\sim 7.5\%$ of the Li^+ ions on interstitials) this coherent intensity amounts to $\sim 10\%$ of the incoherent intensity, in good agreement with the experimental observation (figure 3). The fact that the scattering is predominantly incoherent not only simplifies the interpretation of the experiment, but allowed us to perform subsequent experiments without polarization analysis (and corresponding gain in neutron flux). Note that S has only weak incoherent scattering ($\sigma_{\text{incoh}}(S) = 0.007$ barn [5]).

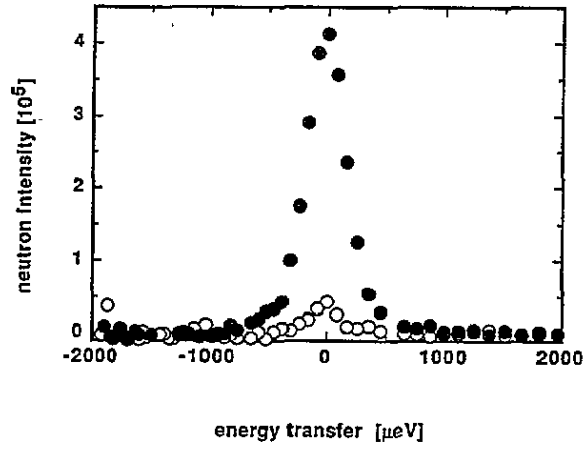

Figure 3. Quasielastic neutron scattering on an Li_2S single crystal, measured with polarized neutrons on the TOF spectrometer D7 at the ILL at $T = 1173$ K: ●, incoherent; ○, coherent.

The variation of the FWHM of the quasielastic peak as a function of the modulus of the scattering vector $|Q|$, as obtained from a preliminary analysis of the data with one Lorentzian, is shown in figure 4. The observed behaviour is typical for a system where jump diffusion (not restricted in space) occurs: the broadening increases initially in proportion to Q^2 and then oscillates at larger $|Q|$.

2.2. *Measurements with a triple-axis spectrometer*

Having confirmed that the scattering is almost purely incoherent, we measured the quasielastic scattering along symmetry directions [100], [110] and [111] using the triple-axis spectrometer IN5 at the reactor Saphir, Würenlingen. All experiments were carried out in a cylindrical resistance furnace placed on a large goniometer head for crystal alignment. The temperature stability was ± 2 K at 1363 K. The spectrometer was used in its doubly focusing (monochromator and analyser) mode of operation [8].

Single-crystal spectra were measured with an energy resolution of 170 μeV using a fixed incoming wavelength of 4.12 Å (4.82 meV energy) and a cooled Be filter. Measurements were taken at temperatures of 300 K (in order to determine the resolution function of the spectrometer when no diffusion takes place), 1173 K, 1273 K and 1363 K. Details of performed scans (Q vectors and temperatures) are given in table 1 and two typical spectra are displayed in figure 5. The range of the energy transfer was restricted to ΔE from -1000 to $+2500$ μeV, so that the broad component of the quasielastic scattering (cf section 3, model

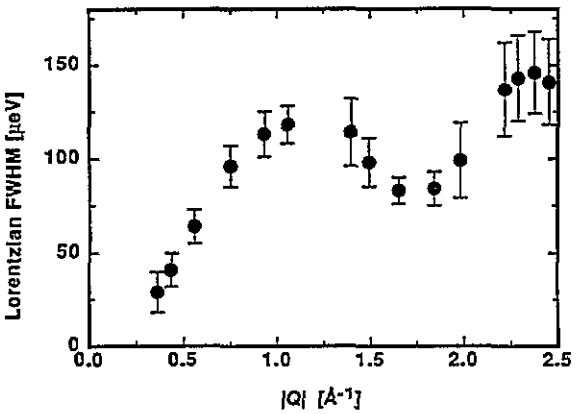

Figure 4. The behaviour of the experimentally determined FWHM of quasielastic scattering as a function of $|Q|$, measured on D7 at 1173 K (one Lorentzian; no model involved).

Table 1. Details of experiments on Li_2S: data used in the fit and derived results. Lattice constant $a_0 = 5.939$ Å (1320 K). Debye–Waller factor $B_{Li} = 5.5 \pm 1.2$ Å^2.

Temperature (K)	1173	1273	1363
Occupation of (8c) site [2]	0.932	0.889	0.824
Single crystal			
spectra along [100]	—	—	6
spectra along [110]	5	—	—
spectra along [111]	4	4	3
$\tau(8c) \rightarrow (4b)$ (ps)	17.3 ± 4.2	6.7 ± 1.5	4.3 ± 0.8
Diffusion constant (10^{-5} cm^2 s^{-1})	1.17	2.89	4.23
Powder			
spectra			5
$\tau(8c) \rightarrow (4b)$ (ps)			3.6 ± 0.4

calculation of mode 3 in figure 7 with a Lorentzian FWHM of approximately 1800 μeV) could not be observed.

The instrumental configuration was therefore changed to an incoming wavelength of 2.44 Å (13.74 meV energy) in conjunction with a graphite filter. The energy resolution was 640 μeV and the accessible range in energy transfer up to $\Delta E = \pm 5000$ μeV. Unfortunately we had a break in the current supply, and rapid cooling led to a crack in the single crystal. The experiments to verify the existence of the broader component of the quasielastic scattering had therefore to be carried out on a 'powder' sample. Data were measured at temperatures of 300 K and 1363 K for $|Q| = 0.6$, 0.8, 1.2, 1.6 and 2.0 Å^{-1}, the spectrum at $|Q| = 1.6$ Å^{-1} is shown in figure 6.

3. The jump diffusion model

In principle, the incoherent quasielastic scattering provides us with the possibility of investigating the motion of a single particle because the scattering law is related to the time dependent self-correlation function [6]. Neutron diffraction data on Li_2S at 1300 K

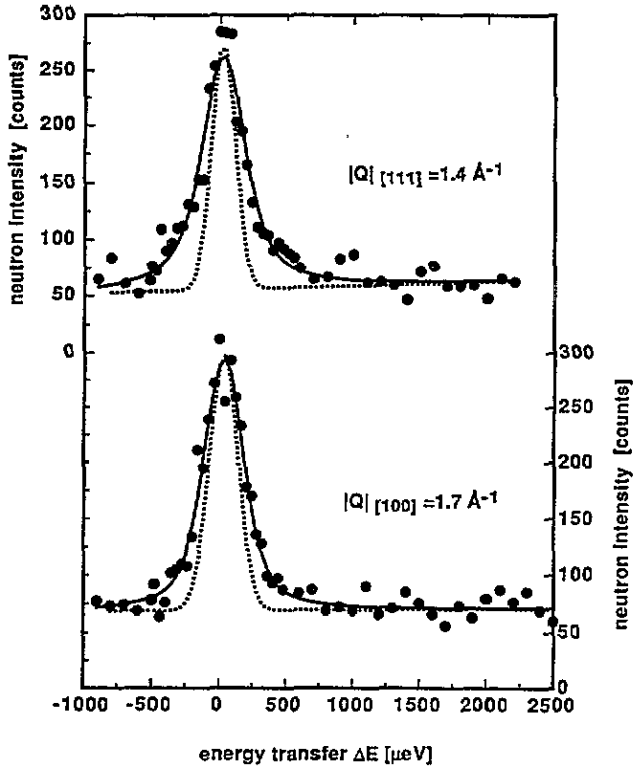

Figure 5. Quasielastic spectra of Li_2S at $T = 1363$ K, measured on the triple-axis spectrometer; incoming wavelength, 4.12 Å: ●, experimental points; ----, 300 K (instrumental resolution); ——, model calculation with residence time $\tau_{(8c)\rightarrow(4b)} = 4.3$ ps.

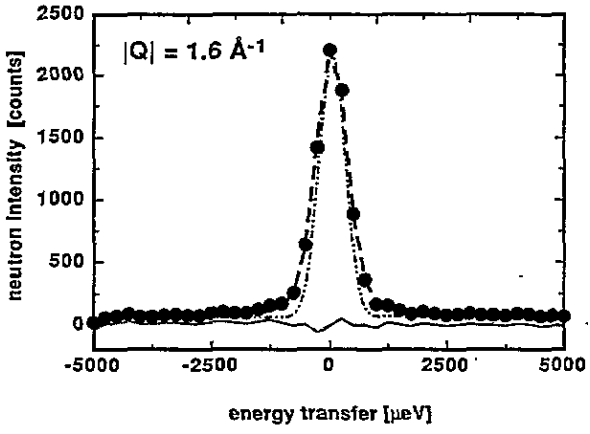

Figure 6. A quasielastic spectrum from a $^7Li_2S$ powder sample measured on the triple-axis spectrometer; incoming wavelength, 2.44 Å: ●, experimental points at 1363 K; – – –, model calculation of Lorentzian mode 3, residence time $\tau_{(8c)\rightarrow(4h)} = 3.6 \pm 0.4$ ps; ----, difference (obs – calc); — · · —, 300 K (instrumental resolution).

indicate that ~ 15% of the Li ions occupy interstitial octahedral sites [2]. Therefore we have analysed our data in terms of an extended Chudley–Elliott jump diffusion model, which allows for jumps from the regular (8c) sites to the interstitial (4b) sites and *vice versa*, without any direct jumps between regular sites; the possible jump vectors are shown in figure 1.

Our model describes the diffusion process by considering three sublattices: the (8c) sites split into two sublattices (labelled 1 and 2) which are tetrahedrally surrounded by (4b) interstitial Li sites (labelled 3). The jump rates are $(\tau_{13})^{-1} = (\tau_{23})^{-1}$ for jumps from regular to interstitial sites and $(\tau_{31})^{-1} = (\tau_{32})^{-1}$ for jumps back to the regular positions. Because these sublattices do not form a Bravais lattice, an extension of the Chudley–Elliott model has to be used [9, 10], as follows.

Writing $P_i(r, t)$ for the probability of finding a diffusing atom at the point r at the time t in the sublattice i the diffusion process is described by a set of coupled rate equations of the form

$$\frac{\partial P_i(r,t)}{\partial t} = \sum_{j,k} \frac{P_j(r + l_{ijk}, t)}{n_{ji}\tau_{ji}} - \frac{P_i(r,t)}{n_{ij}\tau_{ij}} \qquad (1)$$

where n_{ij} is the number of nearest neighbours on the sublattice j to the site i connected to it by the k jump vectors l_{ijk}. We can write three such equations to describe the probability of occupation of each of the sublattices. $(\tau_{ij})^{-1}$ is the jump rate from site i to any of the neighbouring j sites and the mean residence time on a site in the sublattice i is given by

$$\tau_i = \left(\sum_j \frac{1}{\tau_{ij}} \right)^{-1} \qquad (2)$$

The corresponding Van Hove self-correlation function $G_s(r, t)$ [6] is related to the probability functions $P_i(r, t)$ by introducing the boundary conditions

$${}^j P_i(r, 0) = \delta_{ij}\delta(r) \qquad (3)$$

where ${}^j P_i(r, t)$ is the particular solution on the ith sublattice given that the diffusing particle started on the jth sublattice at $t = 0$. The total solution is then given by

$${}^j P(r, t) = \sum_i {}^j P_i(r, t) \qquad (4)$$

so that the self-correlation function $G_s(r, t)$ can be written as

$$G_s(r, t) = \sum_{j=1}^{3} c_j \, {}^j P(r, t) \qquad (5)$$

where c_j is the probability of occupation of the jth sublattice.

Fourier transformation of equation (1) gives in matrix form

$$(\partial/\partial t) I(Q, t) = \mathbf{A} I(Q, t) \qquad (6)$$

where the matrix elements of $\mathbf{A}$ are given by

$$A_{ij} = \frac{1}{n_{ji}\tau_{ji}} \sum_k \exp(-\mathrm{i}Q \cdot l_{ijk}) - \frac{\delta_{ij}}{\tau_i}. \qquad (7)$$

$I(Q,t)$ is the intermediate scattering function related to the neutron incoherent scattering law $S_{\rm inc}(Q,\omega)$ via Fourier transformation [6].

The model allows for two different hopping rates $(\tau_{ij})^{-1}$ from regular sites to interstitial sites and *vice versa*. These hopping rates are related to the occupation factors c_i by the detailed balance condition

$$\tau_{ij} = \tau_{ji}\frac{c_i}{c_j} \qquad \sum_i c_i = 1. \tag{8}$$

Since $\tau_{ij} \neq \tau_{ji}$ the matrix $\mathbf{A}(Q)$ is not Hermitian but may be transformed by a diagonal similarity transformation to give a Hermitian matrix

$$\mathbf{A}(Q)' = \mathbf{T}\mathbf{A}(Q)\mathbf{T}^{-1} \tag{9}$$

where the matrix $\mathbf{T}$ is given by [11]

$$\mathbf{T} = \begin{bmatrix} \sqrt{\tau_{31}/\tau_{13}} & 0 & 0 \\ 0 & \sqrt{\tau_{32}/\tau_{23}} & 0 \\ & 0 & 1 \end{bmatrix}. \tag{10}$$

The solution of equation (6) (with the transformed matrix $\mathbf{A}'$) gives after Fourier transformation

$$S_{\rm inc}(Q,\omega) = \sum_{j=1}^{3} \frac{w_j(Q)a_j(Q)}{|a_j(Q)|^2 + \omega^2}. \tag{11}$$

The scattering law is a sum of three Lorentzians. The halfwidths $a_j(Q)$ are the eigenvalues of the $\mathbf{A}^1$ matrix, and the Q dependent weights $w_j(Q)$ of the Lorentzians are determined by the orthonormal eigenvectors α_{kj} of the matrix and the occupation factors c_i:

$$w_j(Q) = \left| \sum_i \sqrt{c_i}\alpha_{ij} \right|^2. \tag{12}$$

The occupation factors can be estimated from e.g. neutron diffraction data, and there remains only one free parameter in the model, the mean residence time $\tau_{(8c)\to(4b)}$.

The results of a calculation with $\tau_{(8c)\to(4b)} = 4.3$ ps are presented in figure 7, where FWHM and weights along [111] and [100] are plotted. The scattering law is split into three Lorentzian components: mode 1, with an energy width ranging from 0 μeV to a value of ~ 300 μeV; mode 2, which is dispersionless with a constant value of ~ 300 μeV and mode 3, which oscillates around a value of 1800 μeV (and is well separated from the other two modes). Along [111] quasielastic broadening stems from two modes (figure 7(a,b)): mode 1 dominates for Q values smaller than 0.8 Å^{-1} with a corresponding weight > 0.8, whereas in the range of 1.3 Å^{-1} $< Q <$ 2.4 Å^{-1} mode 2 has a weight > 0.8. Thus the broadening is expected to increase with $\sim |Q|^2$ at low Q due to mode 1 and to reach a constant value due to the Q independent mode 2. Mode 3 (with the larger width) is expected to give significant contributions to quasielastic scattering at higher Q values (figure 7(d)).

The scattering law for small Q is determined by only one Lorentzian, which corresponds to the long-range diffusion. The two other Lorentzians have vanishing weights

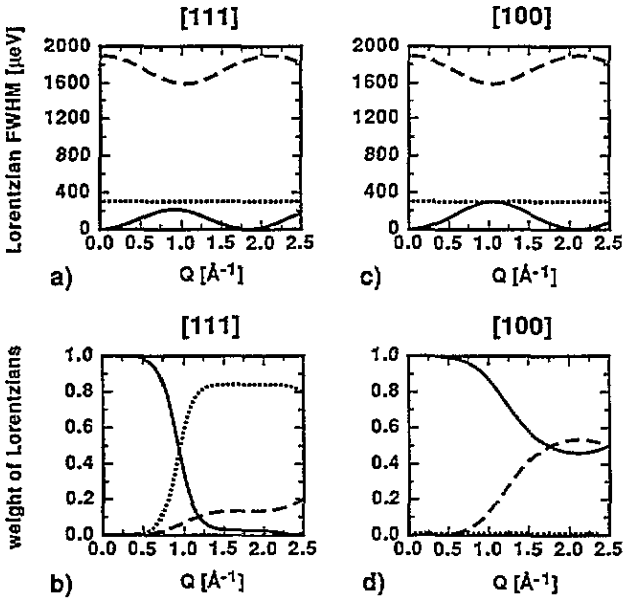

Figure 7. Model calculations of Lorentzian FWHM and Lorentzian weights as a function of Q with residence time $\tau_{(8c)\to(4b)} = 4.3$ ps: ——, mode 1; ----, mode 2; – – –, mode 3. (a) Halfwidths along [111]; (b) weights along [111]; (c) halfwidths along [100]; (d) weights along [100].

(figure 7(b, d)) and the diffusion constant D can be estimated. The analytic expression for D is obtained as follows. **A** defined by (6) and (7) has, for Q parallel to [100], the form

$$\mathbf{A}_{[100]} = \begin{bmatrix} -1/\tau_1 & 0 & A/2\tau_3 \\ 0 & -1/\tau_1 & A/2\tau_3 \\ A/\tau_1 & A/\tau_1 & -1/\tau_3 \end{bmatrix} \tag{13}$$

where $A = \cos(Qa_0/4)$, a_0 is the lattice constant, $\tau_1 = \tau_{13} = \tau_{23}$ and $\tau_3 = \tau_{31}/2 = \tau_{32}/2$. The matrix elements A_{21} and A_{12} are zero due to the fact that the model does not allow direct jumps between regular sites. The halfwidth of the Lorentzian and the diffusion constant D are given by the eigenvalue with unit weight at low Q

$$\Delta\omega(Q) = Q^2d^2/3(\tau_1 + \tau_3) \tag{14}$$

with

$$D = d^2/3(\tau_1 + \tau_3) \tag{15}$$

and the jump distance $d = \sqrt{3}a_0/4$.

It should be noted however that the Chudley–Elliott model is derived in the low concentration limit ($c \to 0$) i.e. where each site in the diffusion path is available and not occupied by another interstitial. The fact that there is a finite concentration of interstitials leads to corrections to the simple model of the form [12]

$$\tau(c) = [1/(1-c)]f(c)\tau(0). \tag{16}$$

The term in square brackets on the right hand side of (16) is a first-order correction to account for the average occupancy whereas the correlation factor accounts for correlated jumps. For example, after an interstitial has made a jump the probability of a return jump is increased due to the higher than average chance (probability) of finding a vacancy in the original position. Although the correlation factor can be calculated [12–14] it has a subtle effect on the quasielastic line shape, which is more difficult to take into account. This arises because the effect of the correlation factor is only seen at long times (i.e. small ω). Thus the quasielastic peak changes from a Lorentzian described by $\tau(c)$ at small ω to a Lorentzian described by $\tau(c)/f(c)$ at large ω.

However in the present case we expect this effect to be small and certainly outside the experimental precision of the measurements. Thus we have ignored the effect of correlation and the residence times given have not been corrected to infinite dilution.

4. Results and discussion

In our model of the Li diffusion process in Li_2S the incoherent neutron scattering law is a superposition of three Lorentzians. The halfwidths of the Lorentzians are rather different, and therefore experiments were carried out using different incoming energies and energy resolutions.

Experimental spectra obtained on the single crystal in the high-resolution mode of operation as well as the corresponding model calculations are shown in figure 5. Significant broadening could be observed along both symmetry directions [100] and [111]. The spectra were fitted using the scattering law (11) convoluted with the experimental resolution functions, which were a good approximation of Gaussian shape. Table 1 summarizes the data used in the fit. The occupation factors of the (8c) sites were taken from previous neutron diffraction experiments [2], and therefore the only free parameter of the model is one residence time. Additional fitted parameters relating the scattering law to the experimental intensities are the Debye–Waller factor (Q dependence) and an overall scale factor.

Experiment and model calculations agree quite well, and features of linewidth and intensity could be well reproduced, in particular the Q independent width of the dominant mode 2 (largest weight) along [111] for $Q > 1.0$ Å^{-1} (figure 8), and also the mode 1 behaviour along [100] (with its Q dependence of the quasielastic broadening and of the observed intensity) (figure 9). The residence time and the diffusion constant as functions of the temperature are given in table 1. At 1363 K we obtain a value of 4.3 ± 0.8 ps for the residence time $\tau_{(8c)\rightarrow(4b)}$.

The investigation of the broad component was carried out using a powder sample, and the scattering law (11) had to be averaged over all possible Q orientations. The quasielastic spectrum measured at $T = 1363$ K at a scattering vector $|Q| = 1.6$ Å^{-1} is shown in figure 6; the observed broadening can well be described in the framework of our model. The fit of the model to the broad component leads to $\tau_{(8c)\rightarrow(4b)} = 3.6 \pm 0.4$ ps, a residence time in satisfactory agreement with the value derived from the high-resolution experiments.

The experimental determination of both components of the quasielastic scattering clearly demonstrates that Li diffusion in Li_2S takes place via interstitial hopping. This result is in contrast to previous work on the isostructural compound Li_2O [15] and on the fluorite systems (e.g. $SrCl_2$ [16]) where diffusion by hopping between regular nearest-neighbour and next-nearest-neighbour sites was invoked. In a simple picture with 'hard spherical ions' a different behaviour of Li_2S compared to the fluorites may be expected. If one considers fluorite like systems, the comparison of the ratio of the ionic radius of the mobile ion to

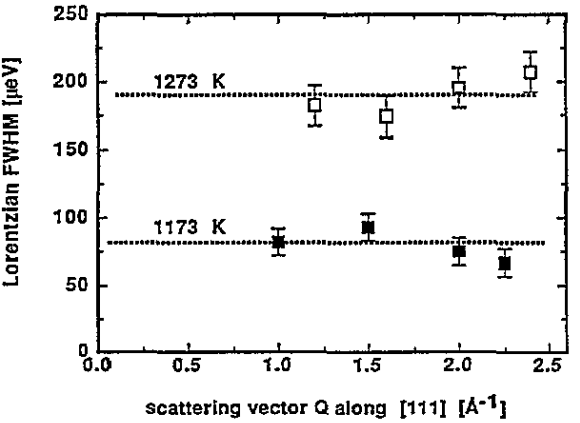

Figure 8. The linewidth of Lorentzian mode 2 along [111]. Experimental points: □, 1273 K; ■, 1173 K. As predicted by the model (figure 4(a)) the width is not Q dependent; fitting of the data leads to $\tau_{(8c)\rightarrow(4b)}$ values of 17.3 ± 4.2 ps at $T = 1173$ K and 6.7 ± 1.5 ps at $T = 1273$ K.

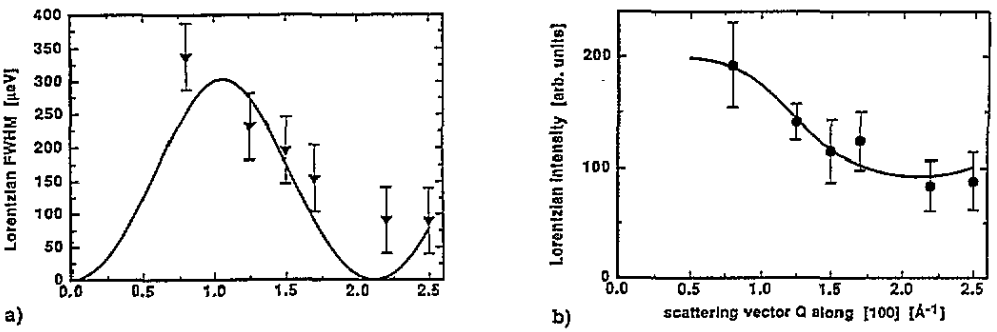

Figure 9. (a) The linewidth of Lorentzian mode 1 along [100]: ▼, experimental points at 1363 K; ——, model calculation with residence time $\tau_{(8c)\rightarrow(4b)} = 4.3$ ps. (b) The intensity of Lorentzian mode 1 along [100]: ●, experimental points at 1363 K; ——, model calculation with residence time $\tau_{(8c)\rightarrow(4b)} = 4.3$ ps.

the radius of the immobile ion ($R = r_m/r_{im}$) is for e.g. $SrCl_2$, $R_{SrCl_2} = (1.81$ Å$/1.10$ Å$) = 1.65$, whereas the corresponding R value for Li_2S is: $R_{Li_2S} = (0.68$ Å$/1.90$ Å$) = 0.36$ (ionic radii [17]). The S^{2-} sublattice can well accommodate the small Li ion in its large interstitial sites, but in the fluorites the mobile ion is larger than the immobile ion so that the occupation of the interstitial 4b site causes strong lattice distortions. In fact, analysis of neutron scattering data of powder and single-crystal samples of fluorites show that instead of interstitial defects, defect clusters of anions and cations are formed [18]. The finite lifetime of these clusters gives rise to coherent quasielastic scattering, which is not observed in the present experiments on Li_2S. Ionic diffusion paths can be discussed following similar geometric arguments: the ionic radius of the S^{2-} sphere is too large to allow an Li^+ ion to perform 'direct' jumps along [100] or [110]; forced by short-range repulsion the Li^+ has to follow a curved path 'around' the S^{2-} ion (figure 1; S^{2-} radius not to scale for clarity) with [111] as the most open direction. Whereas steric arguments based on a model with spherical ions can help in understanding the different behaviour of Li_2S and fluorites, the

comparison of Li_2S and Li_2O (with R_{Li_2O} = (0.68 Å/1.46 Å) = 0.47) is less transparent. A key to the understanding might be in the different electronic polarizabilities α of S^{2-} and O^{2-}. For O^{2-} in Li_2O a value of $\alpha = 2.07$ Å^3 is given; values for S^{2-} are $\alpha = 4.8$–5.9 Å^3 (from refraction data [19]), where a higher α value qualitatively expresses a more extended and complicated electronic structure (e.g. for Li^+, $\alpha = 0.03$ Å^3 [19]). Therefore we summarize that the unique S^{2-} electronic structure gives rise to characteristic behaviour in refraction and in chemical bonding, with a large variety of polysulphides being formed by alkali metals, as well as in in ionic diffusion.

Acknowledgments

The authors wish to thank H G Smith for providing us with the ^7Li isotope for the single-crystal growth. We are grateful to M Koch and R Thut from the LNS and to the furnace group of the ILL for technical assistance. This work was supported by the Nationaler Energie-Forschungs-Fonds, grant 478.

References

[1] Carron P L 1990 *PhD Thesis* University of Geneva
[2] Bührer W, Altorfer F, Mesot J, Bill H, Carron P L and Smith H G 1991 *J. Phys.: Condens. Matter* **3** 1055–64
[3] Mjwara P M, Comins J D, Ngoepe P E, Bührer W and Bill H 1991 *J. Phys.: Condens. Matter* **3** 4289–92
[4] Springer T 1972 *Springer Tracts on Modern Physics* vol 64 (Berlin: Springer) pp 1–99
[5] Sears V F 1992 *Neutron News* **23** 26–37
[6] Squires G L 1978 *Introduction to the Theory of Thermal Neutron Scattering* (Cambridge: Cambridge University Press)
[7] Blank H and Maier B (ed) 1988 *Guide to the Neutron Research Facilities at the ILL* Institut Laue–Langevin, Grenoble
[8] Bührer W 1994 *Nucl. Instrum. Methods* A **338** 44–52
[9] Chudley C T and Elliott R J 1961 *Proc. Phys. Soc.* **77** 353–61
[10] Rowe J W, Sköld K, Flotow H E and Rush J J 1971 *J. Phys. Chem. Solids* **32** 41–54
[11] Kutner R and Sosnowska I 1977 *J. Phys. Chem. Solids* **38** 741–6
[12] Tahir-Kheli R A and Elliott R J 1983 *Phys. Rev.* B **27** 844–57
[13] Ross D K and Wilson D L T 1977 *Proc. IAEA Conf. Neutron Inelastic Scattering (Vienna, 1977)* (Vienna: IAEA) pp 383–97
[14] Kehr K W, Kutner R and Binder K 1981 *Phys. Rev.* B **23** 4931–45
[15] Farley T W D, Hayes W, Hull S, Hutchings M T, Alba M and Vrtis M 1989 *Physica* B **155&156** 99–102
[16] Schnabel P, Hayes W, Hutchings M T, Lechner M T and Renker B 1983 *Radiat. Eff.* **75** 73–7
[17] Kittel Ch 1956 *Introduction to Solid State Physics* 2nd edn (New York: Wiley) pp 81–2
[18] Hutchings M T, Clausen K, Dickens M H, Hayes W, Kjems J K, Schnabel P G and Smith C 1984 *J. Phys. C: Solid State Phys.* **17** 3903–40
[19] Tessman J R, Kahn A H and Shockley W 1953 *Phys. Rev.* **92** 890–5